J. Cell. Mol. Med. Vol 15, No 8, 2011 pp. 1747-1756

Butyrylcholinesterase interactions with amylin may protect pancreatic cells in metabolic syndrome

Shani Shenhar-Tsarfaty [a, #], Tal Bruck [b, #], Estelle R. Bennett [b], Tsafrir Bravman [c], Einor Ben Aassayag [a], Nir Waiskopf [b], Ori Rogowski [a], Natan Bornstein [a], Shlomo Berliner [a], Hermona Soreq [b, *]

[a] *Departments of Neurology and Internal Medicine, Tel Aviv Sourasky Medical Center, Sackler Faculty of Medicine, Tel Aviv University, Tel Aviv, Israel*
[b] *The Institute of Life Sciences and the Interdisciplinary Center of Neuronal Computation, The Hebrew University of Jerusalem, Jerusalem, Israel*
[c] *Bio-Rad Laboratories, Inc., Gutwirth Park, Technion, Haifa, Israel*

Received: April 28, 2010; Accepted: August 23, 2010

Abstract

The metabolic syndrome (MetS) is a risk factor for type 2 diabetes mellitus (T2DM). However, the mechanisms underlying the transition from MetS to T2DM are unknown. Our goal was to study the potential contribution of butyrylcholinesterase (BChE) to this process. We first determined the hydrolytic activity of BChE in serum from MetS, T2DM and healthy individuals. The 'Kalow' variant of BChE (BChE-K), which has been proposed to be a risk factor for T2DM, was genotyped in the last two groups. Our results show that in MetS patients serum BChE activity is elevated compared to T2DM patients and healthy controls ($P < 0.001$). The BChE-K genotype showed similar prevalence in T2DM and healthy individuals, excluding this genotype as a risk factor for T2DM. However, the activity differences remained unexplained. Previous results from our laboratory have shown BChE to attenuate the formation of β-amyloid fibrils, and protect cultured neurons from their cytotoxicity. Therefore, we next studied the *in vitro* interactions between recombinant human butyrylcholinesterase and amylin by surface plasmon resonance, Thioflavine T fluorescence assay and cross-linking, and used cultured pancreatic β cells to test protection by BChE from amylin cytotoxicity. We demonstrate that BChE interacts with amylin through its core domain and efficiently attenuates both amylin fibril and oligomer formation. Furthermore, application of BChE to cultured β cells protects them from amylin cytotoxicity. Taken together, our results suggest that MetS-associated BChE increases could protect pancreatic β-cells *in vivo* by decreasing the formation of toxic amylin oligomers.

Keywords: type 2 diabetes • metabolic syndrome • cholinergic activity • butyrylcholinesterase-K variant

Introduction

The metabolic syndrome (MetS), characterized by abdominal obesity, hyper-triglyceridaemia, low levels of high-density lipoprotein (HDL) cholesterol, hypertension and elevated fasting glucose levels [1] is a major health risk in developed countries, with a prevalence of 25% among adults in the United States [2]. MetS is associated with an increased risk for cardiovascular disease in both genders [3]. It is also perceived as signalling a pre-diabetic state [4] since many of its features are predictors of type 2 diabetes mellitus (T2DM) and the risk for incident T2DM is up to five times higher in individuals with MetS compared to controls [5].

T2DM, inversely, is viewed as an end-stage manifestation of MetS [6], although the molecular mechanisms involved in this shift remain incompletely understood. Over 90% of T2DM patients show extracellular deposits adjacent to β cells [7, 8] formed by aggregation of the islet amyloid polypeptide (IAPP, or amylin), a normal product of β cells co-produced and co-secreted with insulin. Amylin is elevated in conditions associated with insulin resistance and hyper-insulinaemia such as the early stages of

[#]These authors contributed equally to this work.
*Correspondence to: Hermona SOREQ,
Department of Biological Chemistry,
The Hebrew University of Jerusalem,
The Edmond J. Safra Campus, Givat Ram,
91904 Jerusalem, Israel.
Tel.: 972-2-6585109
Fax: 972-2-6520258
E-mail: soreq@cc.huji.ac.il

doi:10.1111/j.1582-4934.2010.01165.x

T2DM, and accumulating evidence supports a role for amylin deposits in T2DM β-cell failure [9–12]. Interestingly, a synthetic analogue of human amylin, SYMLIN® (pramlintide acetate), is used as an adjunct to insulin therapy in both type 1 and type 2 diabetes patients [13] to facilitate improvement in glycaemic control and weight gain [14].

Biochemical and neurophysiological measurements point to enhanced sympathetic and impaired parasympathetic functioning in MetS patients [15]. More specifically, decreased vagal activity was found in individuals with obesity [16], dysglycaemia [17], hypertension [18, 19] and hyperlipidaemia [20], suggesting perturbation of cholinergic pathways in MetS. One possible cause of impaired vagal activity is the increase in butyrylcholinesterase (BChE)-mediated hydrolysis of acetylcholine (ACh) observed in early T2DM patients, followed by BChE decreases in established patients [21]. This temporary BChE elevation would reduce parasympathetic signals, increasing the sympathetic to parasympathetic ratio.

These reported changes in BChE activity have been viewed from an enzymatic point of view. However, we recently discovered that BChE attenuates the formation of Alzheimer's disease (AD) β-amyloid (Aβ) fibrils and protects cultured neurons from their cytotoxicity [22]. We also found that a peptide derived from the C-terminal sequence of BChE-U, the 'usual' variant of the enzyme, was more potent in attenuating this oligomerization than a peptide derived from the C-terminal sequence of BChE-K, the 'Kalow' variant of the enzyme with lowered cholinesterase activity [23]. Interestingly, BChE-K has also been proposed to be a risk factor for T2DM and coronary artery disease [24, 25]. Our Aβ findings raised the possibility that BChE could similarly attenuate the formation of amylin fibrils, so that its transient increase would serve a protective function in delaying the shift from MetS to T2DM. We also surmised that should the enzymatic activity of BChE be involved, the BChE-K variant would be less capable of performing this function.

Materials and methods

Participants

This study involved two cohorts. The first was recruited from apparently healthy working volunteers attending the Tel Aviv Sourasky Medical Center for routine examinations. Participants were classified according to number of MetS components (0–5), and included 429 controls (MetS components <3), 146 MetS and 58 T2DM patients. For genetic analysis a second cohort of T2DM ($n = 56$) and age- and BMI-matched non-diabetic controls ($n = 265$) was recruited from the outpatient clinics of the Medical Centre. Written informed consent was obtained from all participants and approved by the local ethics committee (Numbers 00–116 and 02–049).

Definition of risk factors

MetS definition was based on the National Cholesterol Education Program Adult Treatment Panel III criteria [1] with the modified impaired fasting glucose criteria [26] as proposed by the updated American Heart Association/National Heart, Lung, and Blood Institute scientific statement [27]. Patients were defined as suffering from diabetes mellitus if they displayed blood glucose levels of ≥126 mg/dl at fasting or reported the intake of insulin or oral hypoglycaemic medications. Hypertension was defined as blood pressure of ≥140/90 mmHg in two separate measurements or the intake of antihypertensive medications. Dyslipidaemia was defined as low-density lipoprotein (LDL) or HDL cholesterol higher than recommended levels according to risk profile defined by the updated Adult Treatment Panel III recommendations in persons with triglycerides over 200 mg/dl (>2.26 mmol/l) or use of lipid-lowering medications. Smokers were defined as individuals who smoked at least 5 cigarettes per day, whereas past smokers had stopped smoking at least 30 days before examination.

Clinical laboratory methods

Blood was drawn in the morning after a fasting period of at least 12 hrs. Glucose was determined using an Autoanalyzer (Beckman Instruments, Fullerton, CA, USA). Total cholesterol, HDL cholesterol and triglycerides were determined using a Bayer Advia 1650 chemistry analyser (Bayer Healthcare Diagnostics Division, Newbury, UK). Inter-assay coefficients of variation (CVs) for total cholesterol, triglycerides and HDL were in the range of 4%, 3% and 3%, respectively. The intra-assay variations for these tests were approximately 2%.

Serum cholinesterase analysis

Acetylcholinesterase (AChE) and BChE serum activity levels were assayed in microtitre plates using an adaptation of the Ellman assay [28]. Hydrolysis of acetylthiocholine (ATCh, Sigma, Rehovot, Israel) was followed by spectrofluorometry (Spectrafluor Plus, Tecan, Maennedorf, Switzerland) at 405 nm, after 20 min. pre-incubation with (for AChE activity) or without (for total activity) a specific BChE inhibitor (tetra isopropyl pyrophosphoramide, Sigma). Total cholinergic activity is defined as 'cholinergic status' and total serum hydrolysis of ATCh after subtraction of AChE hydrolytic activity is defined as 'calculated BChE activity'.

Gene polymorphism analysis

Genomic DNA was extracted from nucleated blood cells. For single nucleotide polymorphism analysis a 214 base-pair PCR product was amplified using the forward primer (5′-CTGTACTGTGTAGTTAGAGAAAATGGC-3′, nucleotide −105 to −79 upstream to the intron3/exon4 boundary) and the reverse primer (5′-CTTTCTTTCTTGCTAGTGTAATCG-3′, nucleotides 1709–1686). A fluorescein- labelled anchor probe (5′-CCAGCGATGGAATC-CTGCTTTCC-3′-fluorescein, nucleotides 1628–50) and a LC-Red-640-labelled detection probe (5′-CTCCCATTCTGCTTCATCAATATT-3′-phosphate, nucleotides 1603–26) were used as previously reported [29, 30] .

Proteins and peptides

Recombinant human BChE (rhBChE) was produced and provided by PharmAthene (Montreal, Canada) as described [23]. Recombinant human 'read-through' AChE (rhAChE-R), the monomeric stress-induced isoform

of AChE, was produced and provided by Protalix Biotherapeutics (Carmiel, Israel) [31, 32]. Soybean 15-Lipoxygenase (LOX) was purchased from Cayman Chemical (Ann Arbor, MI, USA). Human amylin (1–37, KCNTATCATQRLANFLVHSSNNFGAILSSTNVGSNTY) was purchased from Bachem (Bubendorf, Switzerland). Peptides corresponding to the C-terminal sequence of human BChE and shown previously to attenuate Aβ oligomerization [23] were synthesized by GenScript Corporation (Piscataway, NJ, USA) as follows: BChE synthetic peptide (BSP)-U (GNIDEAEWEWKAGFHRWNNYMMDWKNQFNDYT, corresponding to the 'usual' variant BChE-U) and BSP-K (as above, with an A6T substitution equivalent to A539T in the full-length protein, corresponding to BChE-K).

Immunoblotting

After separation by SDS-PAGE and transfer to nitrocellulose amylin was visualized using a specific antibody (Abcam, Cambridge, England, ab11022), peroxidase-conjugated goat antimouse IgG (115–035-062, Jackson ImmunoResearch Laboratories, PA, USA) and enhanced chemiluminescence (EZ-ECl, Biological Industries, Beit-Haemek, Israel).

Thioflavine T fluorescence

The assay is based on a shift in the fluorescence excitation spectrum of the benzothiazole dye Thioflavine T (ThT) from 340 to 450 nm upon selective interaction with β-sheet amyloid structures, with fluorescence signals reflecting the amount of amyloid fibrils formed. Amylin was dissolved in hexafluoroisopropanol and incubated overnight at room temperature for monomerization. After hexafluoroisopropanol evaporation under nitrogen amylin was dissolved in distilled deionized water. The assay was performed in white microtiter plates (236108, Nunc, Roskilde, Denmark). Wells contained 12.8 μM amylin, 10 μM ThT and rhBChE, LOX, BSP-U or BSP-K, in 10 mM Tris-Cl, pH 7.4. Fibril formation was monitored by spectrofluorometry (GENios Pro, Tecan) for 25 hrs at 20 min. intervals (excitation, 450 nm; emission, 485 nm). In all experiments ThT was in excess of rhBChE and LOX by a factor of at least 100. This guaranteed that the observed reduction in fluorescence was not due to non-specific binding of ThT to the proteins in a manner that would preclude its binding to amylin, but due to a true reduction in amylin fibril formation.

Surface plasmon resonance (SPR)

The ProteOn™ XPR36 Protein Interaction Array System (Bio-Rad Laboratories, Hercules, CA, USA) was used to characterize protein–peptide interactions. For immobilization to the chip amylin was monomerized as above, resuspended in 100% dimethyl sulfoxide (DMSO) and diluted in acetate buffer pH 5.0 to 0.2 mg/ml. BSP-U and BSP-K were dissolved in 60% DMSO and diluted in acetate buffer pH 3.0 to 0.2 mg/ml. rhBChE and AChE-R were diluted in acetate buffer pH 4.0 to 0.03 mg/ml. IgG (rabbit), which served as a reference protein, was diluted in acetate buffer pH 4.5 to 0.05 mg/ml. Immobilization to a ProteOn General Layer Compact (GLC) chip (Bio-Rad) was carried out by standard amine coupling (RU was typically between 3000 and 6000). For injection over the chip amylin was monomerized and diluted in phosphate-buffered solution containing 0.005% Tween-20 and DMSO, to yield working concentrations of 75.8, 38, 19, 9.5 and 4.7 μM, all containing 3% DMSO.

Photo-induced cross-linking (PICUP)

Samples containing 51.3 μM amylin and 0.52 μM rhBChE or LOX, in 10 mM Tris-Cl, pH 7.4, were incubated at room temperature. At various times aliquots were removed and the soluble fraction recovered by centrifugation (14,000 rpm, 30 min.). Tris (2,2′-bipyridyl) dichlororuthenium (II) hexahydrate ($Ru(II)bpy_3^{2+}$, Sigma) and ammonium persulphate (Bio-Rad) were added (final concentrations of 100 μM and 2 mM, respectively). After 30–60 sec. illumination the reaction was terminated with SDS-PAGE loading buffer containing 5% β-mercaptoethanol. Samples were heated (5 min., 95°C), separated on 16% tris-tricine gels and visualized by silver staining (SilverXpress®, Invitrogen, Carlsbad, CA, USA). The protocol is based on reference [33].

Cell culture and toxicity measurements

The rat insulinoma cell line RINm5F (ATCC, Manassas, VA, USA) was cultured according to supplier instructions. For toxicity measurements 2×10^4 cells/well were plated in white microtitre plates with transparent bottoms (165306, Nunc). After 24 hrs low-serum (1% foetal calf serum) medium containing 25.6 μM amylin and 0.064 μM rBChE or LOX was applied to the cells and 48 hrs later toxicity of the treatments was determined by measuring cell viability (CellTiter-Glo® Luminescent Cell Viability Assay kit, Promega, Madison, WI, USA).

Statistical analysis

Data in the tables are displayed as mean ± S.D. for the continuous variables and as number of patients and percentage for categorical variables. The one-way Kolmogorov–Smirnov test was used to assess the distributions. The difference in mean calculated activities between genotypes was evaluated using Student's t-test; $P < 0.05$ was considered statistically significant. The SPSS statistical package was used to perform all statistical evaluations (SSPS, Chicago, IL, USA).

Results

MetS involves an increase in serum BChE activity

BChE activity was measured in sera from the first cohort (see 'Materials and methods'), comprising 146 MetS patients and 429 healthy individuals. We observed considerably higher circulation BChE activity in the MetS patients in comparison to the controls: 1345.7 ± 368 nmol/min.*ml *versus* 1101.3 ± 348 nmol/min.*ml, respectively ($P < 0.001$, Table 1). This was compatible with the notion of impaired parasympathetic activity in MetS patients due to increased ACh degradation. We noted a gender difference regarding several of the known risk factors for T2DM in this cohort: Men presented higher serum cholinesterase activities than women, accompanied by higher BMI, CRP, systolic and diastolic blood pressure and frequencies of hypertension and dyslipidaemia,

Table 1 Characterization of study participants

	Controls (0) $N = 429$	MetS (1) $N = 146$	*P*-value (0–1)	Diabetes (2) $N = 58$	*P*-value (0–2)
Age, years	43.7 (10.5)	49.1(10)	<0.001	65.5 (11)	<0.001
Gender, %males	56.4	87.0	<0.001	55.2	0.898
BMI, kg/m^2	25.5(4)	29.4 (45)	<0.001	26.7 (4)	0.052
Current smokers, %	17.1	23.0	0.120	13.1	0.718
Calculated BChE activity, nmol substrate hydrolysed/min.*ml	1101.3 (348)	1345.7 (368)	<0.001	1059.8 (218)	0.208
AChE activity, nmol substrate hydrolysed/min.*ml	577.4 (213)	624.9 (183)	0.012	482.4 (113)	<0.001

Comparison of MetS (1) and type 2 diabetes (2) patient characteristics to apparently healthy participants (0). Males and current smokers are presented as percentage and *P*-value was calculated using the chi-square test. All other parameters are presented as mean and S.D. (in parenthesis), compared by Student's t-test for normally distributed variables and the Mann-Whitney U-test for non-normally distributed variables. $P < 0.05$ is considered statistically significant.

(Fig. 1G and H, and Tables S1 and S2). BChE activity, more than AChE activity, was correlated significantly with several dysmetabolism risk factors and tested biomarkers (Table S3). Moreover, patients with more components of the MetS showed significantly higher BChE activities in a component number-dependent manner, in both genders (Fig. 1A–D). This demonstrated the association of parasympathetic impairment with dysglycaemia, hyperlipidaemia, aging, obesity and hypertension. Significant interaction effects were also noted between waist circumference and triglyceride levels, and were shown to reflect increased BChE activity, also following adjustment for age and smoking status (Fig. 1E and F). Another explanation for the elevated BChE in the MetS patients could be an inadvertent bias in patient selection relating to BMI status: previous findings from our group show a positive correlation between BChE activity and BMI status [34, 35]. An additional possible bias is the difference in medication intake between the two groups. These potential biases were not evaluated in the current study, and further longitudinal studies would be needed to assess them.

BChE activity and genotype distribution in T2DM and healthy individuals

The MetS-associated increase in serum BChE activity could be coincidental. Alternatively, it could indicate a feedback response aimed at attenuating the shift from MetS to diabetes. To distinguish between these options we first compared T2DM patients and non-diabetic controls (of the second cohort, see 'Materials and methods'). The calculated serum BChE activity in these two groups was similar (1059.75 $\pm$ 218.1 nmol/min.*ml in T2DM *versus* 1087.1 $\pm$ 217.4 nmol/min.*ml in the non-diabetic controls, $P = 0.386$, Fig. 2A) and lower than that of the MetS group of the first cohort, suggesting that the MetS increase in BChE activity is transient and that a decline in activity occurs during the shift from MetS to diabetes.

The decrease in BChE's hydrolytic activity towards ACh could reflect reduced production and/or a decrease in interaction with various protein or peptide partners. BChE-K, which has an Ala-Thr substitution at position 539 near the C-terminus and shows reduced hydrolytic activity, assisted us in determining between these possibilities. Interestingly, diabetic individuals presented a lower incidence of the BChE-K genotype (76.8% UU, 21.4% UK and 0.3% KK in T2DM patients *versus* 70.9% UU, 24.2% UK and 4.9% KK in healthy controls) although the total of 21.7% carriers in the diabetic group compared to 29.1% carriers in non-diabetics did not differ significantly ($P = 0.156$). We then measured serum BChE activity in BChE-K and BChE-U carriers in the T2DM and non-diabetic groups. Non-diabetic BChE-K carriers showed predictably lower activity than non-diabetic BChE-U carriers (1016.95 $\pm$ 206.2 *versus* 1113.4 $\pm$ 216.6, $P = 0.002$, Fig. 2B, left-hand column). However, diabetic patients of all three genotypes (UU, UK, KK, Fig. 2A and B, right-hand column) showed similarly low activities, regardless of genotype. Together these results suggest that BChE-K is not a risk factor for T2DM.

rhBChE interacts with amylin

To examine the involvement of BChE protein–peptide interactions in the shift from MetS to T2DM, we performed PICUP of highly purified rhBChE of the U variant (Fig. 3A) with the amylin peptide. This method enables the covalent cross-linking of proteins or peptides found in close proximity, without the use of modifications or chemical cross-linkers. Following incubation and cross-linking, the resultant complexes of rBChE and amylin were separated by gel electrophoresis and immune-stained for amylin. A pronounced double band of over 250 kD is seen (Fig. 3C), representing rhBChE

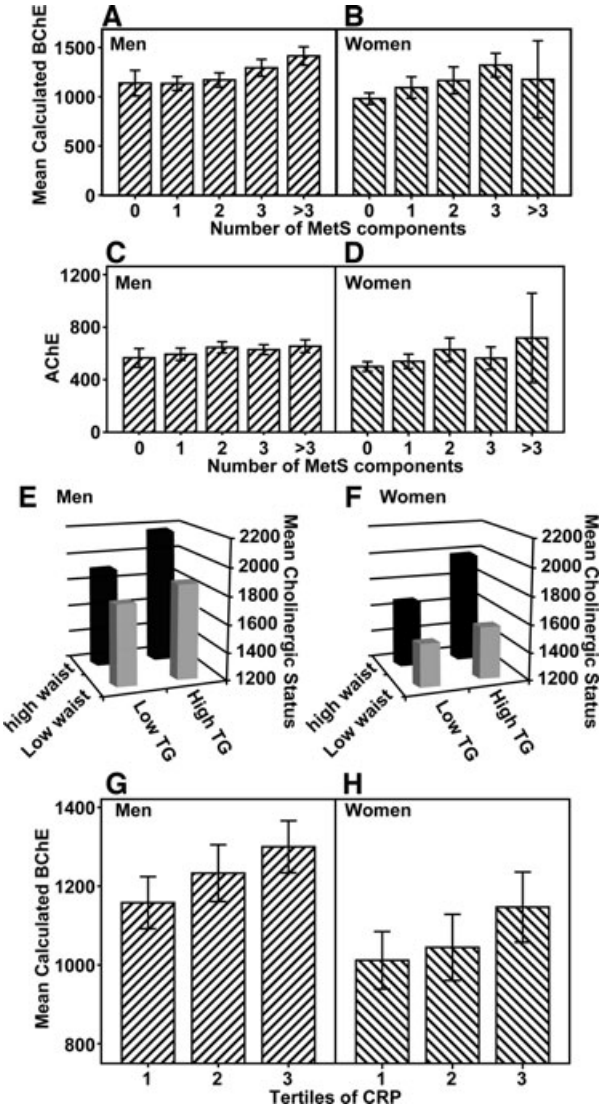

Fig. 1 Cholinergic activity and risk factors in MetS patients. (**A**)–(**D**) Cholinergic activity (**A**–**B**, BChE; **C**–**D**, AChE) *versus* the number of MetS components, according to gender, represented as bar graphs ± S.E.M. (0 represents individuals with no components, >3 represents individuals with four or five components). One-way ANOVA was used to compare groups, $P < 0.001$. (**E**) and (**F**) The interaction of triglyceride levels and waist circumference with cholinergic activity. Bar graphs represent mean cholinergic status ± S.E.M. for each combination of factors, by gender (**E**, men; **F**, women). (**G**) and (**H**) BChE activity in tertiles of C-reactive protein. Bar graphs represent the mean calculated BChE activity ± S.E.M., by gender (**G**, men; **H**, women).

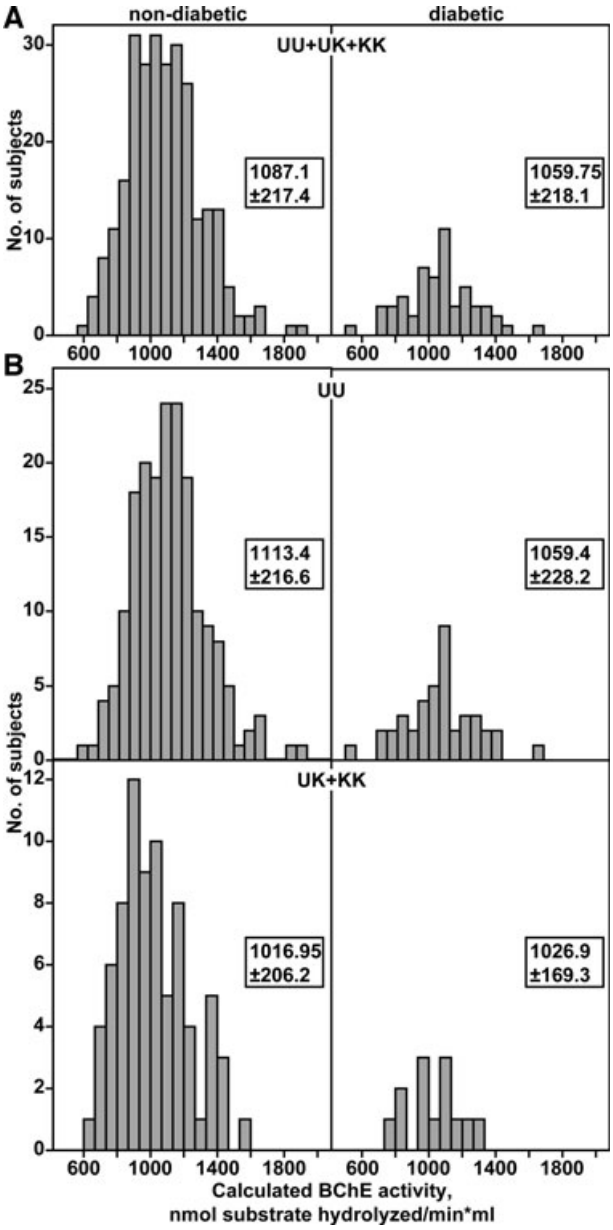

Fig. 2 Serum BChE activities in diabetic and non-diabetic individuals of different genotypes. BChE activity was calculated as detailed in the 'Materials and methods' section, and is expressed as nmol substrate hydrolysed per minute per ml serum. Bar graphs represent the frequencies of activity, and the average activity ± S.D. of each group is noted in the box. (**A**) Activity in diabetic and non-diabetic individuals of all three genotypes (UU, UK and KK) (diabetic, 1059.75 ± 218.1 nmol/min.*ml; non-diabetic, 1087.1 ± 217.4 nmol/min.*ml, $P = 0.386$). (**B**) Activity in diabetic and non-diabetic individuals of genotypes UU *versus* UK and KK. (Diabetic UU, 1059.4 ± 228.2; non-diabetic UU, 1113.4 ± 216.6, $P = 0.146$; diabetic UK+KK, 1026.9 ± 169.3; non-diabetic UU+UK, 1016.95 ± 206.2, $P = 0.87$).

tetramers (~280 kD) complexed with amylin (the doublet may represent two distinct forms of these complexes), as well as an amylin hexamer band (~27 kD). Samples containing rhBChE alone showed no staining for amylin.

We next used SPR to study the interaction between rhBChE and amylin. The sensorgram in Figure 3D shows that amylin (as ana-

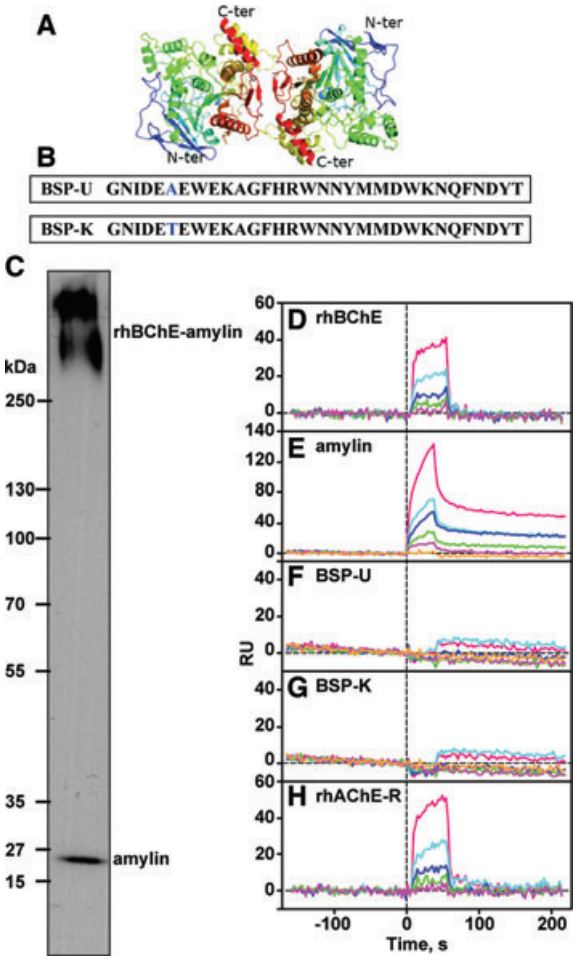

Fig. 3 Direct rhBChE-amylin interactions. (**A**) Cartoon of the human BChE dimer based on a 2.8 Å X-ray structure with each monomer coloured from blue at the N-terminus to red at the C-terminus [50]. (**B**) Sequence of C-terminal peptides BSP-U and BSP-K with the A6T change marked in blue. (**C**) Immunoblot of amylin-BChE complex. Amylin and rhBChE were incubated and the soluble fraction cross-linked as described in 'Materials and methods'. The complex was separated by 8% SDS-PAGE, transferred to nitrocellulose, and amylin was detected using a specific primary antibody, horseradish peroxidase-conjugated secondary antibody and enhanced chemiluminescence. The positions of the molecular mass standards are shown at the left. (**D**) SPR sensorgram showing dose-dependent amylin-BChE interactions. rhBChE was immobilized to a GLC chip and five increasing concentrations of amylin (red, 4.7 μM; green, 9.5 μM; blue, 19 μM; cyan, 38 μM; pink, 75.8 μM) were injected over the chip, in addition to running buffer (yellow). Background (interaction of injected amylin with IgG) was subtracted from all the traces shown. (**E**) Sensorgram showing dose-dependent interactions between amylin immobilized to a GLC chip and amylin injected over the chip. (**F**) Sensorgram showing lack of interaction between immobilized BSP-U and injected amylin: all traces are at background RU and show no dose-dependence. (**G**) Sensorgram showing lack of interaction between immobilized BSP-K and injected amylin. (**H**) Sensorgram showing dose-dependent interactions between immobilized AChE-R and injected amylin. All experiments were carried out at least twice on different days, using different protein and peptide solutions, and the traces shown are representative.

lyte) interacts with immobilized rhBChE in a dose-dependent manner. This interaction could occur through the core domain of BChE, similar to the interaction of the synaptic AChE (AChE-S) with the amyloidogenic peptide Aβ [36]. Alternatively, it could involve its C-terminal area, similar to the interaction of the 'read-through' variant AChE-R and BChE with Aβ [22, 23, 37]. To distinguish between these possibilities we studied the interaction of amylin (as analyte) with the immobilized C-terminal peptides BChE-U and BChE-K (Fig. 3B), as well as immobilized amylin. The resultant sensorgrams revealed dose-dependent amylin–amylin interactions (Fig. 3E), but neither BSP-U nor BSP-K interacted with amylin (Fig. 3F and G). We therefore attribute the observed amylin interaction to the core domain of rhBChE. The SPR measurements also revealed a dose-dependent interaction between amylin and AChE-R (Fig. 3H).

rhBChE attenuates the aggregation of amylin

The similar amyloidogenic properties of amylin and Aβ [38] together with our previous findings that AChE-R can attenuate Aβ fibril formation *in vivo* [37] raised the possibility that rhBChE can similarly attenuate the aggregation of amylin. We therefore used the ThT fluorescence assay to measure the aggregation of amylin in the absence and presence of rhBChE. As shown in Figure 4A, amylin alone yielded a sigmoidal fluorescence time curve, consistent with the presence of lag, elongation and saturation phases in the fibril formation process, and in agreement with previous reports [10, 39]. Addition of rhBChE at increasing concentrations attenuated amylin fibril formation in a dose-dependent manner, reflected as gradually flattening curves with increasingly longer lag phases and lower saturation fluorescence levels, culminating in total prevention of fibril formation by 0.128 μM rhBChE. We next looked at the effect of LOX on amylin fibrillation. A possible role of LOX was proposed in both AD and T2DM: Similarly to BChE, the levels of LOX increase during the course of both these diseases [40, 41]. In addition, blockade of LOX expression can protect cortical neurons from Aβ-induced apoptosis [42] and knockout of LOX in mice can prevent cytokine-induced pancreatic β-cell dysfunction [43]. Intriguingly, as shown in Figure 4B, LOX also inhibited the fibrillation of amylin, albeit in a less potent manner than rhBChE, with a shorter lag phase and shallower elongation curve. The synthetic BSP-U and BSP-K peptides did not attenuate amylin fibril formation at any of the concentrations used (Fig. 4C and D), indicating that in contrast to its effect on Aβ, BChE attenuation of amylin oligomerization does not involve the C-terminal domain.

rhBChE attenuates the early oligomerization of amylin

ThT fluorescence signals reflect the amount of amyloid fibrils formed [44] but do not define their exact oligomeric state. To determine this, we used the PICUP method to cross-link amylin

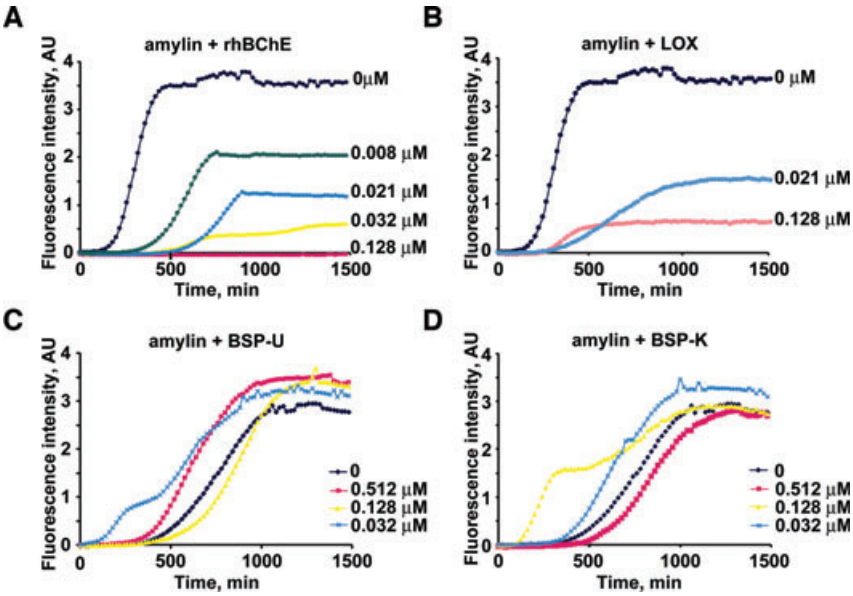

Fig. 4 rhBChE and LOX, but not the BSP-U and BSP-K peptides, affect amylin fibril formation. Proteins and peptides were tested for their effect on amylin fibril formation kinetics by following ThT fluorescence (Excitation, 450 nm; emission, 485 nm) at room temperature for 25 hrs. The concentration of amylin in all experiments was 12.8 μM. The traces shown are representative of three separate experiments. (**A**) Amylin fibril formation in the absence (0 μM) and presence of 0.08 μM, 0.021 μM, 0.032 μM and 0.128 μM rhBChE. A dose-dependent attenuation of fibril formation is observed. (**B**) Amylin fibril formation in the absence (0 μM) and presence of 0.021 μM and 0.128 μM LOX. A less pronounced dose-dependent attenuation of fibril formation is observed. (**C**) Amylin fibril formation in the absence (0 μM) and presence of 0.032 μM, 0.128 μM and 0.512 μM BSP-U. No attenuation of fibril formation is observed. (**D**) Amylin fibril formation in the absence (0 μM) and presence of BSP-K (concentrations as in section **C**). As in the case of BSP-U, no attenuation of fibril formation is observed.

monomers, then separated the resulting oligomeric complexes by SDS-PAGE and visualized them by silver staining. As can be seen in Figure 5A, at the initial time-point (only 3–5 min. after mixing the reaction components) amylin attained several soluble forms, from monomers up to hexamers, reflecting its highly amyloidogeic nature. These soluble forms were not visible, however, at later time-points. When amylin was incubated in the presence of rhBChE it showed similar oligomeric forms at the initial time-point, but these remained in the soluble fraction for at least 12 hrs. In comparison, when amylin was incubated with LOX (Fig. 5B) the oligomeric forms disappeared from the soluble fraction by 6 hrs. Thus, rhBChE prolonged the persistence of small amylin oligomers in solution, whereas LOX accelerated their precipitation out of solution.

rhBChE protects pancreatic β cells from amylin-induced death

We next determined if the *in vitro* effects of BChE on amylin oligomerization are applicable to the viability of cultured pancreatic β cells. We applied amylin, with and without rhBChE or LOX, to cultured pancreatic β cells for 48 hrs, after which cell viability was determined. Addition of amylin to the cells lead to marked cell death, with a calculated IC_{50} of 24 μM for the cytotoxic effect of amylin. However, addition of rhBChE to the cells protected them from the amylin-induced death, increasing cellular viability from 35% to 86%. The presence of LOX had no effect on cell viability, either with or without amylin (Fig. 6A).

Discussion

In our current study we show that BChE activity is elevated in MetS patients whereas T2DM patients show BChE levels similar to those of apparently healthy controls. We also demonstrate that *in vitro*, amylin and highly purified rhBChE interact directly, that rhBChE delays the formation of toxic amylin oligomers, and that it can attenuate amylin fibril formation. Correspondingly, we show that rhBChE can protect cultured pancreatic β cells from amylin toxicity. By combining our clinical findings with our biochemical results, we advance an albeit simplistic but viable hypothesis, that BChE elevation may affect the shift from MetS to T2DM: We propose that the transient MetS-associated increase in serum BChE could protect β cells in these patients by interacting with amylin and decreasing the formation of its toxic oligomers, and that this interaction may occur *via* the core domain of BChE.

Our findings reinforce reports claiming that the toxic form of amylin is a soluble oligomer [45]. The ThT assay, which measures increases in non-soluble protofibrils and fibrils, demonstrated that amylin β-sheet formation was attenuated by both BChE and LOX, but did not pinpoint where in the fibrillation process this inhibition occurred. The cross-linking assay, which visualizes the early stages of soluble oligomer formation, showed suppressed formation of larger amylin oligomers by BChE, unlike LOX, which accelerated this process. This functional difference between BChE and LOX in the amylin fibril formation process is prominently evident in their distinct effects on the toxicity of amylin towards cultured β cells: a protective effect of BChE was seen in its reduction of amylin-induced cell death, whereas LOX lacked this protective effect. We hence propose that the toxic form of amylin is found

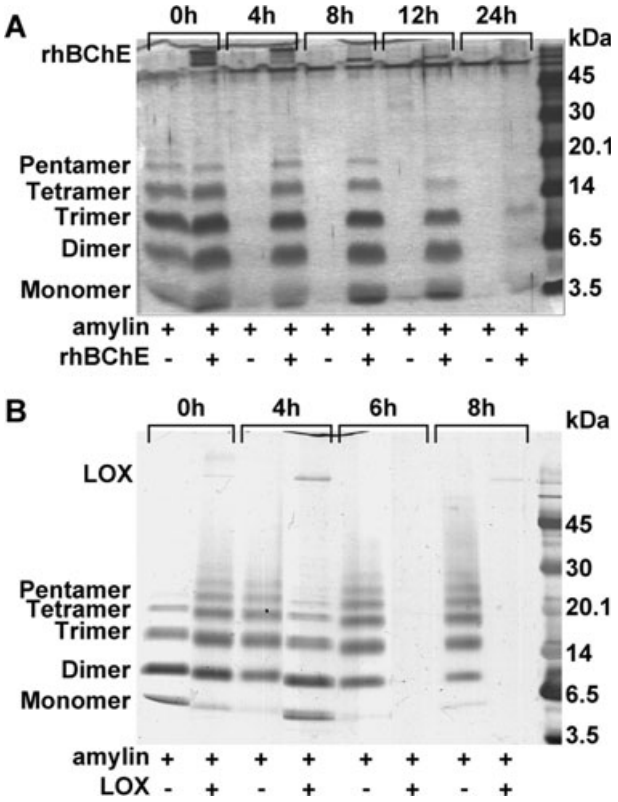

Fig. 5 rhBChE, but not LOX, attenuates clearance of soluble amylin oligomers. Amylin was incubated in the absence and presence of proteins, the soluble phase was cross-linked using the PICUP method, and followed by SDS-PAGE separation and visualization by silver staining. (**A**) 51 μM amylin was incubated for 24 hrs in the absence and presence of 0.52 μM rhBChE, with aliquots removed at 0, 4, 8, 12 and 24 hrs. The gel shows the various oligomeric forms of amylin: the monomer is visible at ~4 kD, and dimers, trimers, tetramers and pentamers are visible at the indicated positions. These forms are seen only in the samples containing rhBChE, visible at the top of the gel. The positions of the molecular mass standards are shown at the right. (**B**) 51 μM amylin was incubated for 8 hrs in the absence and presence of 0.52 μM LOX and aliquots were removed at 0, 4, 6 and 8 hrs. The gel shows the forms of amylin as in (**A**) LOX can be seen as a weak band at the top of the gel.

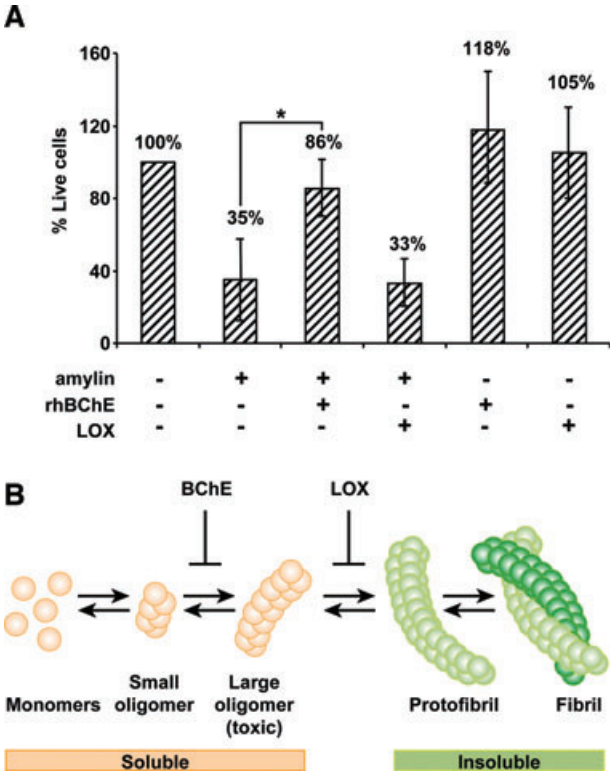

Fig. 6 (**A**) The effect of rBChE and LOX on amylin toxicity in cultured pancreatic β cells. A total of 2×10^4 cells/well were plated and cultured in the presence or absence of 25.6 μM amylin and 0.064 μM rBChE or LOX (molar ratio of 400:1 amylin to protein), and cell viability was determined using the CellTiter-Glo® kit, all as described in 'Materials and methods' . Bar graphs represent the percentage of live cells ± S.D. from three experiments. $^*P < 0.05$, Mann-Whitney test. (**B**) Scheme showing the formation of amylin fibrils from monomers to fully formed fibrils. Monomers and soluble oligomers can be detected by cross-linking, whereas protofibrils and fibrils can be detected by ThT. We propose that BChE and LOX interfere with this process at two distinct points: BChE attenuates the transition between small and large soluble oligomers, the toxic form of amylin, whereas LOX interferes with the formation of protofibrils.

between the points of interference of BChE and LOX in the fibril-formation process, as shown schematically in Figure 6B: BChE attenuates the transition from small to larger soluble oligomers – a stage earlier than that in which the toxic forms are created – thereby preventing the creation of toxic forms and limiting amylin cytotoxicity. LOX attenuates the formation of protofibrils from oligomers – a stage later than that yielding these toxic forms – therefore it does not prevent these forms from being created and does not prevent amylin toxicity.

Although the location of mature amylin fibrils has been shown to be extracellular, the site of initiation of amyloid formation in the pancreas is still under debate, and has been suggested to be both intracellular and extracellular [8]. Thus, the initial small amylin oligomers and the later large amylin oligomers and fibrils, all located extracellularly, would be accessible to elevated levels of plasma BChE. However, as detailed above, we expect serum BChE to interact only with the small oligomers to reduce formation of amylin fibrils.

BChE-K as a risk factor for AD and T2DM has been the subject of much discussion, with studies divided regarding the association between this variant and the diseases [24, 46–51]. In our study we observed a lower incidence of the K-variant in T2DM patients compared to controls. Although we note that the difference was not statistically significant, possibly due to the small sample size, this result excludes the K-variant as a risk factor for T2DM and may even support its proposed protective effect [51].

Our genotype data also support the notion that BChE's role in the shift from MetS to T2DM is a non-catalytic one, reflecting protein–protein interactions rather than enzymatic esterase activity, similar to its function in suppressing Alzheimer's Aβ fibril formation [23]. Finally, our findings that neither BSP-U nor BSP-K affected amylin fibril formation attribute this protective effect to the core domain of BChE.

In conclusion, the dynamically changing levels of BChE during MetS and T2DM that we observed have enhanced our understanding of the genetic and mechanistic processes underlying these syndromes. Our findings suggest that the elevated levels of BChE during MetS can serve as an initial protective mechanism from the cytotoxicity of amylin oligomers towards pancreatic β cells. The possible use of recombinant cholinesterase for delaying type 2 diabetes should hence be considered.

Acknowledgements

We thank PharmAthene, Inc., for the rhBChE, and Protalix Biotherapeutics for the recombinant human AChE-R. This study was supported by a grant from the Israel Science Foundation (399/07).

Conflict of interest

The authors confirm that there are no conflicts of interest.

Supporting Information

Additional Supporting Information may be found in the online version of this article:

Table S1 Healthy and MetS individuals, general information

Table S2 Healthy and MetS individuals, diabetic risk factors

Table S3 Spearman correlations between cholinergic activity and the risk factors in healthy and MetS individuals

Please note: Wiley-Blackwell are not responsible for the content or functionality of any supporting materials supplied by the authors. Any queries (other than missing material) should be directed to the corresponding author for the article.

References

1. **Expert Panel on Detection, Evaluation, and Treatment of High Blood Cholesterol in Adults.** Executive Summary of The Third Report of The National Cholesterol Education Program (NCEP) Expert Panel on Detection, Evaluation, And Treatment of High Blood Cholesterol In Adults (Adult Treatment Panel III). *JAMA.* 2001; 285: 2486–97.
2. **Ford ES, Giles WH, Dietz WH.** Prevalence of the metabolic syndrome among US adults: findings from the third National Health and Nutrition Examination Survey. *JAMA.* 2002; 287: 356–9.
3. **Wilson PW, D'Agostino RB, Parise H, *et al.*** Metabolic syndrome as a precursor of cardiovascular disease and type 2 diabetes mellitus. *Circulation.* 2005; 112: 3066–72.
4. **Najarian RM, Sullivan LM, Kannel WB, *et al.*** Metabolic syndrome compared with type 2 diabetes mellitus as a risk factor for stroke: the Framingham Offspring Study. *Arch Intern Med.* 2006; 166: 106–11.
5. **Cornier MA, Dabelea D, Hernandez TL, *et al.*** The metabolic syndrome. *Endocr Rev.* 2008; 29: 777–822.
6. **Laaksonen DE, Lakka HM, Niskanen LK, *et al.*** Metabolic syndrome and development of diabetes mellitus: application and validation of recently suggested definitions of the metabolic syndrome in a prospective cohort study. *Am J Epidemiol.* 2002; 156: 1070–7.
7. **Kahn SE, Andrikopoulos S, Verchere CB.** Islet amyloid: a long-recognized but underappreciated pathological feature of type 2 diabetes. *Diabetes.* 1999; 48: 241–53.
8. **Hull RL, Westermark GT, Westermark P, *et al.*** Islet amyloid: a critical entity in the pathogenesis of type 2 diabetes. *J Clin Endocrinol Metab.* 2004; 89: 3629–43.
9. **Hoppener JW, Ahren B, Lips CJ.** Islet amyloid and type 2 diabetes mellitus. *N Engl J Med.* 2000; 343: 411–9.
10. **Konarkowska B, Aitken JF, Kistler J, *et al.*** The aggregation potential of human amylin determines its cytotoxicity towards islet beta-cells. *Febs J.* 2006; 273: 3614–24.
11. **Muoio DM, Newgard CB.** Mechanisms of disease: molecular and metabolic mechanisms of insulin resistance and beta-cell failure in type 2 diabetes. *Nat Rev Mol Cell Biol.* 2008; 9: 193–205.
12. **Rhodes CJ.** Type 2 diabetes - a matter of beta-cell life and death? *Science.* 2005; 307: 380–4.
13. **Holman JR.** FDA Approves new adjunct treatment for glucose control. *DOC NEWS.* 2005; 2: 9.
14. **Buse JB.** Metabolic side effects of antipsychotics: focus on hyperglycemia and diabetes. *J Clin Psychiatry.* 2002; 63: 37–41.
15. **Straznicky NE, Eikelis N, Lambert EA, *et al.*** Mediators of sympathetic activation in metabolic syndrome obesity. *Curr Hypertens Rep.* 2008; 10: 440–7.
16. **Alvarez GE, Beske SD, Ballard TP, *et al.*** Sympathetic neural activation in visceral obesity. *Circulation.* 2002; 106: 2533–6.
17. **Thalamas C, Galitzky J, Senard JM, *et al.*** Glucose-induced sympathetic activity and energy expenditure during acute alpha2-adrenergic antagonism in obese subjects. *Int J Obes Relat Metab Disord.* 2000; 24: 695–700.
18. **Esler M.** The sympathetic system and hypertension. *Am J Hypertens.* 2000; 13: 99–105S.
19. **Greenwood JP, Stoker JB, Mary DA.** Single-unit sympathetic discharge: quantitative assessment in human hypertensive disease. *Circulation.* 1999; 100: 1305–10.

20. **Shishehbor MH, Hoogwerf BJ, Lauer MS.** Association of triglyceride-to-HDL cholesterol ratio with heart rate recovery. *Diabetes Care.* 2004; 27: 936–41.
21. **Rao AA, Sridhar GR, Das UN.** Elevated butyrylcholinesterase and acetylcholinesterase may predict the development of type 2 diabetes mellitus and Alzheimer's disease. *Med Hypotheses.* 2007; 69: 1272–6.
22. **Diamant S, Podoly E, Friedler A, *et al.*** Butyrylcholinesterase attenuates amyloid fibril formation *in vitro*. *Proc Natl Acad Sci USA.* 2006; 103: 8628–33.
23. **Podoly E, Shalev DE, Shenhar-Tsarfaty S, *et al.*** The butyrylcholinesterase K variant confers structurally derived risks for alzheimer pathology. *J Biol Chem.* 2009; 284: 17170–9.
24. **Hashim Y, Shepherd D, Wiltshire S, *et al.*** Butyrylcholinesterase K variant on chromosome 3 q is associated with type II diabetes in white Caucasian subjects. *Diabetologia.* 2001; 44: 2227–30.
25. **Vaisi-Raygani A, Rahimi Z, Entezami H, *et al.*** Butyrylcholinesterase K variants increase the risk of coronary artery disease in the population of western Iran. *Scand J Clin Lab Invest.* 2008; 68: 123–9.
26. **Genuth S, Alberti KG, Bennett P, *et al.*** Follow-up report on the diagnosis of diabetes mellitus. *Diabetes Care.* 2003; 26: 3160–7.
27. **Grundy SM, Cleeman JI, Daniels SR, *et al.*** Diagnosis and management of the metabolic syndrome: an American Heart Association/National Heart, Lung, and Blood Institute Scientific Statement. *Circulation.* 2005; 112: 2735–52.
28. **Ellman GL, Courtney D, Andres VJ, *et al.*** A new and rapid colorimetric determination of acetylcholinesterase activity. *Biochem Pharmacol.* 1961; 7: 88–95.
29. **Gatke MR, Viby-Mogensen J, Rosenstock C, *et al.*** Postoperative muscle paralysis after rocuronium: less residual block when acceleromyography is used. *Acta Anaesthesiol Scand.* 2002; 46: 207–13.
30. **Gatke MR, Viby-Mogensen J, Bundgaard JR.** Rapid simultaneous genotyping of the frequent butyrylcholinesterase variants Asp70Gly and Ala539Thr with fluorescent hybridization probes. *Scand J Clin Lab Invest.* 2002; 62: 375–83.
31. **Geyer BC, Muralidharan M, Cherni I, *et al.*** Purification of transgenic plant-derived recombinant human acetylcholinesterase-R. *Chem Biol Interact.* 2005; 157: 331–4.
32. **Meshorer E, Toiber D, Zurel D, *et al.*** Combinatorial complexity of 5′ alternative acetylcholinesterase transcripts and protein products. *J Biol Chem.* 2004; 279: 29740–51.
33. **Fancy DA, Kodadek T.** Chemistry for the analysis of protein-protein interactions: rapid and efficient cross-linking triggered by long wavelength light. *Proc Natl Acad Sci USA.* 1999; 96: 6020–4.
34. **Ben Assayag E, Shenhar-Tsarfaty S, Ofek K, *et al.*** Serum cholinesterase activities distinguish between stroke patients and controls and predict 12 month mortality. *Mol Med.* 2010; 16: 278–86.
35. **Sklan EH, Lowenthal A, Korner M, *et al.*** Acetylcholinesterase/paraoxonase genotype and expression predict anxiety scores in Health, Risk Factors, Exercise Training, and Genetics study. *Proc Natl Acad Sci USA.* 2004; 101: 5512–7.
36. **Inestrosa NC, Alvarez A, Perez CA, *et al.*** Acetylcholinesterase accelerates assembly of amyloid-beta-peptides into Alzheimer's fibrils: possible role of the peripheral site of the enzyme. *Neuron.* 1996; 16: 881–91.
37. **Berson A, Knobloch M, Hanan M, *et al.*** Changes in readthrough acetylcholinesterase expression modulate amyloid-beta pathology. *Brain.* 2008; 131: 109–19.
38. **Glabe CG, Kayed R.** Common structure and toxic function of amyloid oligomers implies a common mechanism of pathogenesis. *Neurology.* 2006; 66: S74–8.
39. **Goldsbury C, Goldie K, Pellaud J, *et al.*** Amyloid fibril formation from full-length and fragments of amylin. *J Struct Biol.* 2000; 130: 352–62.
40. **Yao Y, Clark CM, Trojanowski JQ, *et al.*** Elevation of 12/15 lipoxygenase products in AD and mild cognitive impairment. *Ann Neurol.* 2005; 58: 623–6.
41. **Antonipillai I, Nadler J, Vu EJ, *et al.*** A 12-lipoxygenase product, 12-hydroxyeicosatetraenoic acid, is increased in diabetics with incipient and early renal disease. *J Clin Endocrinol Metab.* 1996; 81: 1940–5.
42. **Lebeau A, Terro F, Rostene W, *et al.*** Blockade of 12-lipoxygenase expression protects cortical neurons from apoptosis induced by beta-amyloid peptide. *Cell Death Differ.* 2004; 11: 875–84.
43. **Han X, Chen S, Sun Y, *et al.*** Induction of cyclooxygenase-2 gene in pancreatic beta-cells by 12-lipoxygenase pathway product 12-hydroxyeicosatetraenoic acid. *Mol Endocrinol.* 2002; 16: 2145–54.
44. **LeVine H, 3rd.** Thioflavine T interaction with synthetic Alzheimer's disease beta-amyloid peptides: detection of amyloid aggregation in solution. *Protein Sci.* 1993; 2: 404–10.
45. **Ferreira ST, Vieira MN, De Felice FG.** Soluble protein oligomers as emerging toxins in Alzheimer's and other amyloid diseases. *IUBMB Life.* 2007; 59: 332–45.
46. **Panegyres PK, Mamotte CD, Vasikaran SD, *et al.*** Butyrycholinesterase K variant and Alzheimer's disease. *J Neurol.* 1999; 246: 369–70.
47. **Lepienski LM, Alcantara VM, Souza RL, *et al.*** Variant K of butyrylcholinesterase and types 1 and 2 of diabetes mellitus. *Chem Biol Interact.* 2005; 157–158: 374–5.
48. **Lehmann DJ, Nagy Z, Litchfield S, *et al.*** Association of butyrylcholinesterase K variant with cholinesterase-positive neuritic plaques in the temporal cortex in late-ons*et Al*zheimer's disease. *Hum Genet.* 2000; 106: 447–52.
49. **Johansen A, Nielsen EM, Andersen G, *et al.*** Large-scale studies of the functional K variant of the butyrylcholinesterase gene in relation to Type 2 diabetes and insulin secretion. *Diabetologia.* 2004; 47: 1437–41.
50. **Grubber JM, Saunders AM, Crane-Gatherum AR, *et al.*** Analysis of association between Alzheimer disease and the K variant of butyrylcholinesterase (BCHE-K). *Neurosci Lett.* 1999; 269: 115–9.
51. **Alvarez-Arcaya A, Combarros O, Llorca J, *et al.*** The butyrylcholinesterase K variant is a protective factor for sporadic Alzheimer's disease in women. *Acta Neurol Scand.* 2000; 102: 350–3.